IJCRT.ORG ISSN : 2320-2882

INTERNATIONAL JOURNAL OF CREATIVE RESEARCH THOUGHTS (IJCRT)

An International Open Access, Peer-reviewed, Refereed Journal

REVIEW ON SYNTHESIS OF METAL DOPED METAL OXIDE NANO-COMPOSITES BY SOL-GEL METHOD TO EXAMINE PHOTO-CATALYTIC ACTIVITY TO DISTINGUISH DIFFERENT ORGANIC-INORGANIC CONTAMINANTS

Altaf Rajani[1], Tejveer Singh Anand[2], Pranav Dave*[3]

[1,2,3] Institute of Research and Development, Gujarat Forensic Sciences University, Gandhinagar –382007, India,

Abstract: In recent study, there are many researches going on to degrade different organic and inorganic contaminants from the wastewater by doing photocatalytic activity. Nowadays, many photocatalysts are using to degrade pollutants. Many conventional researches are reported about using nanocomposites as a photocatalyst. The photocatalytic oxidation of organic-inorganic compounds with nanocomposites as a photocatalyst has been widely premeditated and many achievements have been made. Many synthesis methods of metal nanocomposites have been reported; therein the sol-gel technology is a simple and accurate method to synthesis very fined and crystalline nanoparticles. It has various and valuable properties like reactivity, high melting point and boiling point, hardness, ductility, electronegative property and ionisation energies, electric and thermal conductivity and closely packed structures, which can be apply in various disciplines of research areas. Nanocomposites are used as a photocatalyst for decomposing organic and inorganic compounds due to its high photocatalytic activity, chemical and physical inertness and photochemical stability and reactivity. In this review paper, the synthesis processes of different metal oxide based nanocomposites have been explained with their different characterisation studies to degrade various pollutants from organic-inorganic compounds. There are diverse arrays of using different nanocomposites to degrade pollutants by using photocatalytic activity.

Keywords: - metal oxide; nanocomposites; sol-gel method; photocatalytic activity.

I. INTRODUCTION

Metal oxide Nano-composites plays a very important role in many areas of chemistry, physics and material science. Nanocomposites are those materials with a nanoscale structure which improves the microscopic property of the products. The properties of nano-composite materials do not depend only on the properties of their individual parents but also on their morphology and interfacial characteristics. Nano-composites can be defined as combination of one or more separate components of nanomaterials in order to obtain the best properties of each component. Nano-composites have new applications in many fields such as mechanically reinforced light weight component, non-linear optics, nano-wires, sensors and other system. In technological applications, oxides are used in the fabrication of microelectronic circuits, sensors, piezoelectric devices, fuel cells, coating for the passivation of surface against corrosion and as a catalyst. Metal oxide nano-composites can have unique physical and chemical properties due to its limited size and high density of corner or edge surface sites. Synthesis of different metal oxide Nano-composites with the use of different methods like Co-precipitation method, Sol-gel method, Microemulsion technique, Solvothermal method and Template/Surface derivatized method. The physical, chemical and biological properties of nano-composites are different from the properties of individual atoms and molecules or bulk matter [1],[2],[3],[4]. Nano-composites can improve properties like:

- Mechanical properties including strength, modulus and dimensional stability
- Electrical conductivity
- Decreased gas, water and hydrocarbon permeability
- Flame retardancy and reduced smoke emission
- Thermal stability and heat distortion temperature
- Chemical resistance

Nowadays, Nano-composites are widely used in research areas and provide benefits in future also: Drug delivery system, Anti-corrosion barrier coating, Lubricants and scratch free paints, new fire retardant materials, new scratch/abrasion resistant materials, Superior strength fibers and films [5]. Different types of nano-composites are mainly used in industrial areas like MgO and other alkaline earth oxides are widely used in chemical industry as a scrubber for air pollutant gases and as a catalyst support. ZrO can be used as a structural ceramic, solid electrolyte, gas sensor and as a catalyst. Varieties of Nano-composites have depending upon the types of matrix used and they are classified into three different categories as polymer matrix nano-composites, ceramic matrix nano-composites and metal matrix Nano-composites [6],[7]. Metal oxide Nano-composites are used in various important areas like detection of pesticides and toxins in food beverages, detection of organic and inorganic pollutants in water, drug detection [8],[9]. They are also used in Forensic science is most effective used in the discipline of forensic toxicology for examination of different toxic materials from numerous important forensic evidences like hair, blood, saliva, vitreous humor and even from remains of body skeleton and samples of evidences of fingerprint. And also used to detection of heavy chemicals in organic foods. Nano-composites are also used for biomedical application such as tissue engineering, drug delivery, cellular therapies. Because of unique interactions between polymer and nanoparticles, a range of property combinations can be engineered to mimic native tissue structure and properties [10],[11].

II. METHODOLOGY

2.1 Synthesis process of Nano-composites by Sol-gel method

Nano-composites are synthesizing by different methods like sol-gel method, micro-emulsion method, simple chemical method, solvo-thermal method and vaporization method. Here the sol-gel method is explained and with help of that method how we can synthesize Zn doped TiO_2, Cr doped TiO_2 and Zr doped TiO_2 are explained with different literature survey. The sol-gel process is a wet-chemical technique for the fabrication of materials, employing low temperature, starting either from a chemical solution or colloidal particles to produce an integrated network. In general, sol-gel process can be regarded as the preparation of the sol, gelation of the sol and removal of the solvent [12].

Synthesis process of Zn doped TiO_2

Pawar M.J. and Nimbalkar V.B (2012) synthesized Zn doped TiO_2 nanoparticles with help of sol-gel method. In brief they used titanium isopropoxide, zinc nitrate and cerium nitrate as metal sources. The appropriate amount of titanium isopropoxide was added to the equimolar mixture of citric acid, ethylene glycol and glucose. The molar ratio of citric acid/titanium isopropoxide and citric acid/ethylene glycol was kept constant at 2:1 and 1:1 respectively. This mixture was kept on magnetic stirrer at 60°C for 1hr. The dopant stoichiometry was controlled by mixing to titanium salt solution. The above stirred solution was further heated at 85°C to get the mixture in gel form. Put the gel in muffle furnace at 270°C. For calcination process, put the powder into muffle furnace for few hours at around 500°C [13]. Same as Shuo Pang et al. (2016) implemented sol-gel method to synthesis Zn doped TiO_2 nanocomposites. They used 2.6mL of zinc chloride solution (33mg in 5mL Milli-Q water) and 4mL of acetic acid in solution of 3mL of Milli-Q water and 12mL of ethanol. After that they put the solution on the stirrer for better mixing the solutes and solvents to each other. Then make another solution of titanium isopropoxide (16mL) and ethanol (40mL). Now drop wise mix this solution into upper solution slowly and stir it overnight. The gel is occurred at the end of the process. To convert it into powder form, put the gel in muffle furnace for 12 hours at 120°C and followed the wash with Milli-Q water. For calcination process, put the powder into muffle furnace for few hours at 180°C to 200°C [14]. Guoguang Liu et al. (2005) studied synthesis process of Zn doped TiO_2 by sol-gel method. A solution was made from tetrabutyl titanate and isopropanol in an appropriate proportion and its pH was adjusted to about 3 with HCl. Zinc nitrate was added drop wise via vigorous stirring to the above solution, and the molar ratio of tetrabutyl titanate:isopropanol:deionized water:zinc nitrate was maintained as 1:22:4:0.005. Then a transparent solution was obtained and it was left to get a gel after few minutes. The gel was dried at 80°C until a complete dry gel was obtained, and then dry gel was put in muffle furnace for calcinated at 500°C for 2 hours to convert it into powder form [15]. Similarly, Y.S. Tamgadge et al. (2018) studied synthesis process by simple one step sol gel method. For synthesis of 1% Zn doped TiO_2 Nano-particles, they took 0.0371gm zinc acetate was added in the solution containing Titanium tetra isopropoxide and ethanol, put this solution on stirrer and stirrer continuously. The gel was obtained after the addition of water under constant stirring at 70 – 80 °C for 3 hours. And then gel was put in muffle furnace for calcination process [16].

Synthesis process of Zr doped TiO_2

Replacing the zirconium on the place of zinc, the Nano-composite is giving different properties and it has different applications. Zr doped TiO_2 nanocomposite, which was explained by Saraschand Narnginti et al. (2015) by adding 3.5mL of titanium isopropoxide in 25mL of HPLC grade isopropanol with 100mL of Milli-Q water and leave it for 15minutes on the stirrer. Make another solution by mixing zirconyl nitrate (850mg) in Milli-Q water (2mL). After putting 1hour on the stirrer, the solution was added to the main solution. Now add 3mL of hydrazine hydrate into the solution, so the solution colour was changed from transparent to yellow with some precipitation. For better result of the particles, put the solution into sonicate machine for 90minutes and followed the calcination process in muffle furnace for 24hours at 450°C [17]. Likewise, Jingsheng Wang et al. (2013) were studied synthesis process of Zr doped TiO_2 by simple sol-gel method. At room temperature, a certain amount of $ZrOCl_2$ was added into 50mL of anhydrous solution of ethanol. Then put this solution in stirrer so it will mixed properly, then 15mL of tetrabutyl titanate and 3mL of deionized water were added dropwise into the ethanol solution. To the pH value of above mixture was 0.8, by adding concentrated HCl. The prepare gel was dried at 100°C for 10hours and gel is converted into powder form. A series of zirconium doped TiO_2 catalysts with different concentration of zirconium were prepared by changing amount of $ZrOCl_2$ added in the ethanol solution. Pure TiO_2 NPs were prepared with the same procedure, but without adding $ZrOCl_2$ [18].

Same as Bifen Gao et al. (2010) were followed multi step sol-gel process to synthesis Nano-composite. In this process metallo-organic chemicals were used as precursors. 15mL titanium isopropoxide was mixed with 152.8mL ethanol solution containing 1.8mL H_2O and 1mL HCl and put this solution on stirrer with slowly adding zirconium propoxide solution. The mixture was stirred for another 1hour. Then 1.8mL deionized water was added for further hydrolysis and condensation. The obtained solution was magnetically stirred in the fumehood with a loose cover to evaporate the solvent at room temperature and it turned into transparent gel after stirring overnight. The gel was dried in the oven at 80°C for 1day, then the gel was converted into fine crystal powder and calcinate it into muffle furnace at 500,600 and 700 °C for 1hour to obtain the final product [19]. Tania Bigdeli and Shahram Moradi Dehaghi (2017) studied Zr doped TiO_2 by sol-gel method. At first stage, Titanium Tetra-isopropoxide was dissolved in absolute ethanol with molar ratio of TTIP to ethanol (1:75) and put this solution in a stirred for 15minutes in order to get a precursor solution; after that we added a 0.1g Hydroxy Propyl Cellulose as a stabilizer, and the mixture was continuously stirred for 15minutes to obtain a yellow transparent solution. After that, a mixture of absolute ethanol, nitric acid and CTAB with molar ratio of (0.47, 0.0044 and 0.00028 respectively) was added drop wise into solution 1 during 30minutes by fast stirring to get a transparent solution. This solution was aged at room temperature for 48hours to form a gel. Then, it was heat treated for 30minutes at 100°C to remove the solvent. And it was calcinated in muffle furnace at the 525°C for 24hours. TiO_2 NPs were prepared. Zr doped TiO_2 were prepared by the same method, but difference is that preparation of (solution 2), in this step Zirconium Tetrachloride dissolved in absolute ethanol with the molar ratio of Zr to ethanol (0.0001:1.52, 0.0002:1.52, 0.0003:1.52 and 0.0004:1.52 respectively) added to solution 2. After that, process is repeated as mentioned before and fine particles were prepared easily [20].

Synthesis process of Cr doped TiO_2

Biswajit Choudhury and Amarjyoti Choudhury (2013) studied synthesis process of Cr doped TiO_2. Chromium doped TiO_2 nanoparticles with different concentration of chromium 1.5mol%, 3mol% and 4.5mol%. These nanoparticles were prepared by sol gel method with titanium isopropoxide and chromium nitrate non hydrate as the host and dopant precursors. 6mL titanium isopropoxide and 15mL of 2-propanol were mixed together and put this solution on stirrer. After 20minutes, few drops of water were added to hydrolyze the titanium isopropoxide. A white thick solution was obtained, to which dopant was added drop wise continuously. When all the dopant solutions were added, the hydrolyzed mixture of host and dopant precursor was stirred for 5hours. After that, reaction was stopped and left unstirred for 10-12hours. The reaction mixture was centrifuged with water and ethanol to remove nitrate impurities and then dried in a vacuum oven at 80°C to get the amorphous product [21]. Also, Yan-Hua Peng et al. (2012) studied the process by synthesizing TiO_2 solution with help of butyl titanate as precursor, chromium nitrate as source of Cr metal, ethanol as solvent and acetylacetone as chelate respectively. Stock solution was prepared by appropriate amount of acetylacetone were dissolved in ethanol, and 5wt% glycerol aqueous solution were added to increase the viscosity of the solution. Put this solution in a magnetic stirrer for 35°C and add drop wise butyl titanate in above stock solution. As the mixture solution was homogenous and clear, appropriate amount of water and ethanol was slowly added drop wise under stirring. After being continuously stirring of 30-45minutes, the stable and homogeneous solution with Cr concentration of 0-0.3M was obtained. This solution were dried at 100°C for several minutes to promote the gelation, and this powder was calcinated at 500-700 °C for 1hour to get the final product [22].

Same as Chien-Cheng Pan and Jeffrey C.S. Wu (2006) were formed Cr doped TiO_2 synthesis process followed by sol-gel method. Chromium chloride was used as a precursor and is completely dissolved in ethanol, then mixed into titanium butoxide. The volume of ethanol was 10 times of titanium butoxide and the amount of chromium chloride was calculated based on the desired Cr/Ti ratio. The mixed solution was added slowly drop by drop in a 0.1M HCl solution with 10 times of ethanol/titanium solution volume and quickly hydrolyzed due to large amount of water. During this process the solution was kept cooled at 0°C in a bath by circulating chilled water. The hydrolysis was completed after 8hours, and the solution was dried at 110°C and converted into powder form. And it was calcinated at 400°C for 30minutes [23]. Cheng Wang et al. (2012) studied Cr doped TiO2 Nanoparticles by sol-gel method. Natural zeolite powder was mixed with double distilled water and heated up to 70°C. $TiCl_4$ solution and $CrCl_3$ solution, both was added drop wise into the above solution and pH of the dispersion was adjusted to about 2.0. Put this solution in magnetic stirrer at 70°C for 4hours. After ageing for 12hours, the solution was repeatedly washed with double distilled water to remove the impurities and then dried at 80°C for 2hours. The above sample was finally calcinated in muffle furnace at 200-600°C for 2hours to obtain the natural zeolite Cr doped TiO_2 photocatalyst [24].

2.2 Nano-composite as a Photo-catalyst

Cheng Chen et al. (2007) were synthesized Zn doped TiO_2 Nano-composites. In this photochemical reaction, the photodegradation of dye (20mg/I) was carried out in a jacketed column quartz reactor (700mL). A mercury lamp with high pressure (300W) was placed in a quartz tube which was placed inside the reactor. Use a catalyst concentration of 1gm/I and this reaction was put in a 25°C, maintained by circulating water in the annulus of the reactor. Now, 2mL of solution were collected for subsequent analysis of mass spectrometry [25]. Similarly, Thanh Binh Nguyen et al. (2012) were studied Zn doped TiO_2 Nano-particles and analyzed photo-catalyst activity. Methylene Blue is commonly used chemicals in the chemical and biological industries. Also, it was chosen as a model pollutant. The photocatalytic activity of Zn doped TiO_2 was carried out by measuring the decomposition of an aqueous methylene blue solution ($Co=1\times10^{-5}$ M). Adsorption for 20minutes in the dark, after that four surrounding 20W black-light blue lamps ($\lambda max=352nm$, 0.16A) were activated, and at different time of interval withdraw 3.5mL samples over 240minutes and placed into different filters and syringe. The methylene blue concentration was characterized by UV-vis Spectrophotometer at $\lambda_{max}=666nm$ and residual percentage of methylene blue was calculated by the following equation,

$$MB=\frac{C}{Co}\times100\ \% \qquad (2.1)$$

Where, C_0 and C are initial concentration of MB and concentration at the irradiation time [26]. Ibrahim Elmehasseb et al. (2020) synthesized Zn doped TiO_2 nanoparticles. This photocatalytic degradation process is done under the illumination of 500W tungsten halogen lamp which covers all the visible light range. For continuation of constant light intensity output, the lamp should be turn on before the process by 10-15minutes. In the degradation process of (5ppm) methylene blue dye, the process was done under the variable doses in the neutral medium to stimulate the natural environment. To gave the dose of 7mg to the maximum degradation performance in

the degradation of methylene blue. Detoxification of waste water by the degradation of (3ppm) ciprofloxacin and reduction of (7ppm) of toxic form of Cr(VI) followed by the same condition [27]. Same as, Charline M. Malengreaux et al. (2014) were used Zn doped TiO_2 as a catalyst and composed of Nano-crystallites of anatase with range of 6-7nm. The measured dopant content correspondence to a Zn(II):Ti(IV) mole ratio is equal to 0.5%. Zn doped TiO_2 catalyst is a purely microporous, with a specific surface area and specific microporous volume is equal to $195m^2g^{-1}$ and $0.13gcm^{-3}$. Zn doped TiO_2 catalyst has direct and indirect band gap value of 3.10eV and 2.85eV respectively. Performed the different photocatalyst tasted under the same experimental condition, this catalyst has the highest activity at 298K, after 7hours under UV-vis illumination. The concentration of 4-Nitrophenol measured as a function of reaction, make five initial concentration of 4-Nitrophenol and for studied at each temperature respectively [28].

N. Prabhakarrao et al. (2016) studied of photo-catalytic degradation of Ethylene Blue by photo-catalytic activities of the synthesized catalyst under visible light irradiation. Photocatalytic reaction were done in an photoreactor system in the presence of visible light source (High pressure 400W mercury vapour lamp with a 450nm) and maintained 20cm distance between light source and reaction vessel. The vessel of the reaction is surrounded with water system to keep the photocatalytic reaction system at specific temperature and to absorb the IR radiation. The changing concentration of degraded compound is analyzed by UV-2200 UV-Vis spectrophotometer. The efficiency of photodegradation activity was reported by plotting C/C_0 versus irradiation time (min), where C_0 and C are ethylene blue dye concentration at zero time and time t respectively. The value of C/C_0 was taken as the ratio A/A_0, i.e. the absorbance of the solution at λmax at time t divided by the absorbance at time zero (for EB λ_{max}=520nm).

$$\text{Photodegradation \%} = \frac{A0-At}{A0} \times 100 \qquad (2.2)$$

Where, A_0 and A_t correspondence to the initial absorbance and absorbance at time t respectively [29]. Derya Kapusuz et al. (2013) studied Zr doped TiO_2 nanoparticles. This experiment was performed in a closed vessel container preventing daylight to pass through. A 100W UV lamp was used as a light source. Testing solution were prepared by addition of 0.3gm of undoped, doped and co-doped TiO_2 powder to 300mL aqueous methylene blue solution with an initial concentration of 10 mg/ml. Before starting the test, powder containing MB solution was magnetically stirred in a dark for 30minutes to establish the absorption-desorption equilibrium. Then the solution was irradiated under UV light with constant stirring rate of 500rpm. After 60minutes of irradiation, 3mL of supernatants were taken from the suspension by a syringe filter (pore size 0.22 µm) to scan the UV-vis absorption spectrum, between the range of 200-800nm. The change of absorbance intensity at 664nm under the UV irradiation was calculated with respected to time [30].

Similarly, Chan-Soo Kim et al. (2012) also studied the photo-degradation process of each photo-catalyst by under the photo-reactor chamber. In this experimental set up, we can use gas supply device, photo-degradation reactor and gas chromatograph. The catalyst was prepared by coating of 5mL isopropanol suspension of the photo-catalyst onto glass plate with dimension of 7.5cm × 5cm. These glass plates with catalyst coating were dried at 25°C for 1hour. And then this plate is placed in a quartz reactor, which was kept in a dark and maintained at room temperature. During the evaluation of photo-catalysis, around one to four lamps were illuminated to vary light intensity. Both UV (F8T5/BLB, 8W) and visible (G8T5, 8W) light sources are used to compare photo-catalytic reactivity under each condition. Prepared solutions of toluene and xylene at initial concentration 5ppm in air were introduced into quartz reactor at a flow rate of 550mL/min. The photo-catalyst was stabilized by gas flow for 160minutes. Toluene and xylene both are allowed to reach adsorption equilibrium with the photo-catalyst in the reactor prior to light irradiation. The concentration of toluene and xylene were measured at a time of 40minutes interval over a period of 240minutes using a GC-FID [31].

Same as Baoqing Duan et al. (2018) are working on the synthesis process of Zr doped TiO_2. The photo-catalytic activity are carried out by prepared Na-Zr/TiO_2 photo-catalyst were synthesized by the degradation of formaldehyde under visible light. The photo-catalytic test of the catalyst was performed in a cube reactor with volume of 216L, which was composed of conventional light-transmissive glass. A 25W energy saving light lamp was placed in a center of the reactor with height of 30cm from the bottom. With the help of injection needle, a quantitative formaldehyde solution is injected into the glass reaction chamber; we can diffuse the formaldehyde solution for a certain period of time to uniformly disperse in the glass chamber with the help of wind spin controller. The initial concentration of formaldehyde in the range from 1.0 to $1.2mg/m^3$, which was quantified by formaldehyde meter and the sample, was loaded in the glass plate with diameter of 10cm. The degradation efficiency of formaldehyde was calculated by the following equation,

$$\text{Ƞ} = (C_0 - Ct)/C_0 \times 100\ \% \qquad (2.3)$$

Where, Ƞ is the removal efficiency, C_0 is initial concentration of formaldehyde and Ct is residual concentration of formaldehyde [32]. Hong Zhu et al. (2014) studied preparation and photo-catalytic activity of Cr doped TiO_2 Nano-roads with Nano-cavities. The anatase TiO_2 particles were uniformly with 10M NaOH (70mL) in a 100mL Teflon-lined stainless steel autoclave. The different amount of $Cr(NO_3)_3 \cdot 9H_2O$ were added (the molar ratio of Cr/Ti are 1%, 3%, 5% and 10% respectively). The autoclave was put in oven and heated to 180°C for 48hours, and then followed by the HNO_3 washing. After being dried at 80°C, the product was heated in air at 650°C for an hour. The photo-electrochemical properties of this TiO_2 Nano-roads and commercial anatase TiO_2 particles were further differentiate in three-electrode system with the aid of electrochemical workstation CHI (660B), using the FTO covered by the sample thin film, platinum electrode and saturated calomel electrode as the working electrode, auxiliary electrode and reference electrode, respectively. The Hg lamp (~ 8mW) was used for UV illumination and the sample size was 1.0 × 1.0 cm^2 [33]. Similarly, E.D. Jeong et al. (2013) synthesized Cr doped TiO_2 Nano-particles. To evaluate the photo-catalytic activity of these materials under visible light (λ > 420nm), the oxidative decomposition is occur from isopropyl alcohol (IPA) in gaseous form. But, doped and pure TiO_2 showed the activity for IPA degradation to CO_2. In the case of TiO_{2-x} N_x and doped TiO_2, the concentration of CO_2 increased rapidly with increasing radiation time. The photo-catalytic activity of Cr doped TiO2 for IPA degradation is similar to that of $TiO_{2-x}N_x$. The Cr doped TiO_2 Nano-composites showed much higher decomposition rates and activities then those of Cr/Fe doped TiO_2 for IPA degradation. Thus, the material co-doped with Cr it gives two time higher photo-catalytic activity for photodecomposition of IPA gases than Cr doped particles under visible light [34]. Yan-Hua peng et al. (2012) studied visible-light absorption and photo-catalytic activity of Cr doped TiO_2 Nano-crystal films. The photo-catalytic activity of these films was carried out by photo-catalytic degradation of methyl orange. During the degradation process, it has been shows that the degradation efficiency continuously increasing. Moreover, Cr doped TiO_2 provides much

higher efficiency for methyl orange photo-degradation, it indicate that the Cr doping could greatly improve the photo-catalytic activity of TiO_2 [22].

III.CHARACTERIZATION STUDY

Structural Properties of Nano-composites

Nano-particles/Nano-composite can exhibit unique physical and chemical properties and have received increasing attention & recognition for various applications. Many oxides have wide band gaps and a low reactivity. A decrease in the average size of an oxide particle does in fact change the magnitude of the band gap with strong influence in the conductivity and chemical reactivity [35]. Due to the unique and tunable properties of these metal oxides such as optical, optoelectronic, magnetic, electrical, mechanical, thermal, catalytic, photochemical etc. made themselves excellent candidates for various high level technological applications. Metal oxides are used in various fields like environmental remediation, solar cell, nano-electric device, biological uses, sensors, clean energy production, photovoltaic application [36],[37]. Photocatalytic degradation/detection of various kinds of hazardous materials is using semiconductor powder as photocatalyst. Relatively high photocatalytic activity, biological and chemical stability, low cost, non-toxic nature and long-term stability TiO_2 has been widely used as photocatalyst. Result shows doped TiO_2 is more efficient than pure TiO_2 at photocatalytic activities. Photocatalysis has been applied to decompose waste and toxic materials produced in daily life and in the global environment. And further it is used for degradation process [38],[39]. Structural properties can be studied by the X-ray diffractometer (XRD), FT-IR and SEM/TEM study. The structural properties of zinc oxide doped titanium dioxide, zirconium doped titanium dioxide and chromium doped titanium dioxide were characterized by X-ray diffractometer (XRD), advance diffractometer with Cu-Kα radiation having wavelength 1.54Å. Figure 1 shows the XRD pattern of (a) Zn doped TiO_2, (b) Zr doped TiO_2 and (c) Cr doped TiO_2 nanocomposites. The left hand side graph shows the XRD pattern of Zn doped TiO2. The graph shows different diffraction peaks, which conclude the (101), (004), (200) and (105).

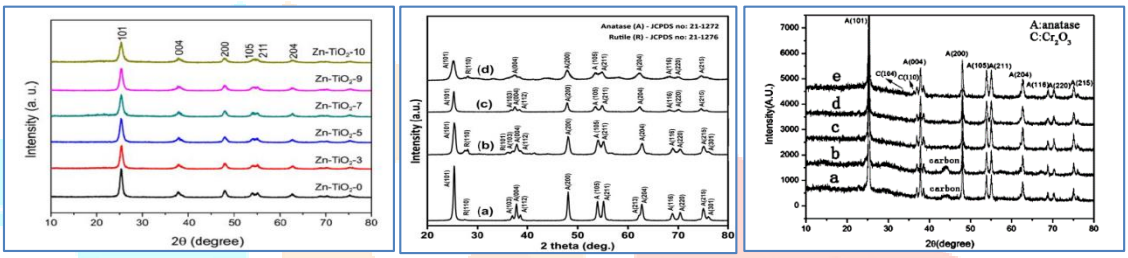

Figure.1 XRD pattern of (a) Zn doped TiO_2, (b) Zr doped TiO_2, (c) Cr doped TiO_2

Cheng Chen et al. (2007) and Thanh Binh Nguyen et al. (2011) studied XRD pattern of Zn doped TiO_2. Here, (200) single diffraction peak shows the presence of zinc in nanocomposite. The molar ratio of Zn doping in TiO_2 was increased, and the crystalline particle size were remains same therefore slightly changes will occur in the graph. The (200) diffraction peak explained the wurtizite structure of zinc material. Other diffraction peaks (101) and (004) show the rutile structure of TiO_2. The content of zinc material in nanocomposite is very less due to low diffraction peak of (200). But the content of TiO_2 is more due to high intense peak of (101) [25],[26]. Similarly, Ibrahim Elmehasseb et al. (2020) and Charline M. Malengreaux et al. (2014) concluded about XRD pattern of Zn doped TiO_2 nanocomposites that the prepared TiO2 is mainly in anatase phase with a sharp peak of 25.2°, in addition to peak at 37.6°, 48.0°, 54.9° and 62.6°. There is a kind of similarity between the patterns due to few drops of impurities [27],[28].

Derya Kapusuz et al. (2013) studied the content of Zr doped TiO_2 and pure TiO_2, which is more due to high and intense diffraction peak of (101), but the diffraction peak (105) shows the anatase structure if TiO_2.The first pattern in XRD graph is of pure TiO2 and the third pattern shows the diffraction peak of Zr doped TiO_2. Same as before explained, here the diffraction peak (200) shows the hexagonal structure of the zirconium. Both the nanocomposites have TiO_2 because of (101) diffraction peak [30]. Chan-Soo Kim et al. (2012) premeditated about XRD pattern of TiO_2, Zr doped TiO_2 nanocomposites and it exhibits diffraction peaks for the anatase and/or rutile phases. The TiO_2 catalyst showed both here anatase and rutile phases. The Zr doped TiO_2 catalyst showed the tetragonal anatase phase of ZrO_2, which indicates that the anatase to rutile phase transformation did not occur. The overall peak intensities of anatase TiO_2 of Zr doped TiO_2 catalyst decreased because insertion of the second metal, which indicates that the addition of zirconium which effectively suppress the growth of TiO_2 crystals and stabilize their structure [31].

N. Prabhakarrao et al. (2016) and Baoqing Duan et al. (2018) characterized the XRD pattern of Zr doped TiO_2. The lattice of TiO_2 is changing the addition of Zr or any other metal, the diffraction angle and crystal particle size were also calculated. After doping of Zr into TiO_2 the diffraction angle reduced from 25.28° to 25.13°, and the crystal particle size become bigger from 11.8nm to 28.2nm. As for Zr doped TiO_2 (2.5%) sample, the diffraction angle of 25.21° and crystal particle size of 27.6nm were obtained, all sample can have anatase structure and no impurity peak were obtained, indicating that Zr^{+4} ions entering into TiO_2 lattice [29],[32]. Hong Zhu et al. (2009) explained the XRD pattern of Cr doped TiO_2. This figure shows the anatase crystalline phases, having diffraction line of (101), (004), (200), (105), (211) and (204) planes at 2θ value of 25.3°, 37.8°, 48.0°, 53.9°, 55.1° and 62.7° respectively. The (101) diffraction peak shows presence of TiO_2 and other diffraction peak shows the presence of chromium in nanocomposite [33].

E.D. Jeong et al. (2008) they studied XRD pattern of pure Cr doped anatase TiO_2 nanoparticles. The entire sample shows the anatase structure of TiO_2. The lattice parameter of anatase TiO_2 with a tetragonal crystal structure was estimated to be a=b=3.78Å and c=9.49Å [34]. Same as, Yan-Hua Peng et al. (2010) calibrated that Cr ions can be dissoluble in the TiO_2 matrix as Cr can be symmetrically substituted to the Ti ions in the Cr doped sample without change of the host TiO_2 matrix. The XRD peak of Cr doped TiO_2 can be obtained at high concentration of Cr and it is in rutile phase. Since the radius of Cr^{+3} ions is very close to that of Ti^{+4} ions, the substitution of Cr^{+3} to Ti^{+4} would not change the rutile lattice. As the mixture of anatase and rutile phase has been found in the 0.05M Cr

doped sample, it may shows that the strain at the anatase/rutile phase. The thin film is doping with 0.05M Cr it contains the mixture of anatase and rutile phase, while TiO_2 thin film is doping with 0.2 or 0.3M Cr shows the pure rutile phase. This result indicating that the Cr doping is the phase transition from anatase to rutile phase and effectively reduced the transition temperature of anatase to rutile phase TiO_2. Scherrer formula was used to calculate the average crystallite size (d) of the sample.

$$d=\frac{0.9\lambda}{\beta\cos\theta_B} \qquad (3.1)$$

Where λ, θ_B and β are the X-ray wavelength (1.54056Å), Bragg diffraction angle and line width at half maximum of the most dominant peak, respectively [22]. Ibrahim Elmehasseb et al. (2020) fabricated the nanocomposites. The figure 2 shows the FTIR Spectra of fabricated nanocatalysts TiO_2 and Zn doped TiO_2, Zr doped TiO_2 and Cr doped TiO_2. The FTIR Spectrum of TiO_2 nanoparticles represent a band near 500cm^{-1} it refers to a bending vibration band of Ti-O-Ti. The stretching band of Zn-O appears at 470cm^1. That causes broadening of the peak between 450cm^{-1} and 650cm^{-1} as a result of doping Zn. The peak at 1650cm^{-1} is corresponding to the bending vibration mode of -OH group. Broadband appears between 3400-3650cm^{-1} it shows the presence of water in TiO_2 surface. This broadband is referring to the hydroxyl peak. Both stretching and bending peak intensities are increased as a result of doping by Zn respectively, and it records the more identification of surface of the doped catalyst and enhancement of the absorption properties [27].

Similarly, K. Kaviyarasu et al. (2016) studied FTIR spectrum of Zn doped TiO_2 nanocrystals in the wavelength range of 3500-500cm^{-1}. Metal oxides have more than one oxygen atom are bound to a single metal atom they usually absorb in the region 1050-870cm^1. The Ti-O and Zn-O stretching vibrations are found in the region of 980-300cm^{-1}. In this case, the spectra of entire sample showed similar peak which is observed at 1579, 1398, 1050 and 980cm^{-1}. The last two bands with weak intensity are assigned to Ti-O and Zn-O symmetric stretching vibration. There are many peaks observed at lower end of the spectrum which are also assigned to Ti-O and Zn-O bending vibrations. Stretching vibrations are observed at 1100, 850, 780 and 610cm^{-1} [40]. Same as A. Stoyanova et al. (2012) analyzed the composition with higher content of TiO_2 (90mol%), several bands are observed: band in the range 610-530cm^{-1}; band at 460cm^{-1} and such at 410cm^{-1} with a shoulder at 430cm^{-1}. And it could be related to the vibration of ZnO_4 polyhedra. The IR spectrum of another composition (50mol% TiO_2) is totally different. The bands in the absorption range 700-400cm^{-1} and it could be related to the vibration of TiO_6 units, comprising both TiO_2 modification (anatase and rutile). The observed intense band at 420cm^{-1} is typically only for rutile. The weak band near 450cm^{-1} could be related to the Ti-O stretching vibration in $ZnTiO_3$ [41].

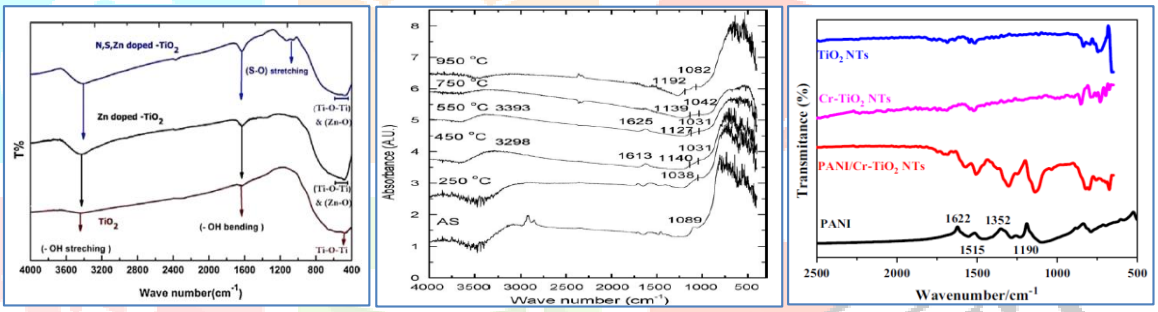

Figure.2 FTIR spectra of (a) Zn doped TiO_2, (b) Zr doped TiO_2, (c)Cr doped TiO_2

FTIR spectra of Zn-TiO_2 after heat treatment the broad peak lying at 400-900cm^{-1} are characteristics vibration peak of [TiO_6] ligands, which are attributed to the asymmetric stretching vibration and bending vibration of Ti-O bond, Li-Ying QIAO et al. (2015) analyzed the peak of Zn-O vibration bond at around 462cm^{-1} and the peak of 1640cm^{-1} are H-O-H bending vibration, related to the constitution water; and the peak at 3000-3400cm^{-1} are from stretching vibration of the surface hydroxyl group of O-H, it is generated by the free water; and the peak at 3837.77cm^{-1} are Ti^{3+}-O-H vibration absorption belonging to the -OH vibration area. As the temperature of heat treatment rises, the broad absorption peak around 3000-3400cm^{-1} get sharper, which is -OH stretch vibration peak of absorption water, therefore there are still -OH groups existing in the Zn-TiO_2 surface [42]. Similarly, Sue-min Chang et al. (2009) examined the FTIR spectra of TOPO capped Zr doped TiO_2, which calcinated at various temperature. The C-H stretching absorption (2768-2981cm^{-1}) which was obvious in the TOPO capped sample disappeared after calcinated at 250°C. C=C or C=O stretching modes at 1320-1790cm^{-1} were observed, which indicates thermal induced partial oxidation and pyrolysis of TOPO. The calcinated sample can shows the OH bending and stretching absorption at 1613 and 3285cm^{-1} respectively. The blue absorption is shifted to 1625 and 3393cm^{-1} at 550°C. The OH absorption was diminished gradually because sample is calcinated above 750°C and disappeared at 950°C. The two absorption band at 1031-1082 and 1127-1192cm^{-1} corresponding to the antisymmetric/symmetric O-P-O stretching bond appeared at the sample was calcinated above 450°C [43]. Also, Tania Bigdeli and Shahram Moradi Dehaghi (2017) showed the FTIR spectra of TiO_2 and Zr doped TiO_2 Nano photo catalyst with various trace amount of Zr. Wave number range from 400-4000cm^{-1} were found. Bending stretching vibration of O-Ti-O, Ti-O-Ti, Zr-O-Ti, O-Zr-O and Zr-O-Zr was in the range of 530-675cm^{-1} and H-O-H in 1615cm^{-1} and stretching vibration was shown in Ti-O, Zr-O, Zr-OH and Ti-OH in 890-1260cm^{-1} [20].

According to Marc Estruga et al. (2010) inspected the FTIR spectra of Zr doped TiO_2, some organic traces remained in the as-prepared titania sample, the typical band observed to the adsorbed glycine appeared at 1409, 1340 and 1120cm^{-1}. C and N elemental analysis it has been determined that the amount of Gly was adsorbed on the surface was nearly 2.5wt%, regardless the presence of dopant. The presence of these organic impurities was not a hindrance to photocatalytic activity. Organic residues were completely eliminated after annealing treatment (spectra not shown) [44]. Kun Yang et al. (2014) examined the FTIR spectra of TiO_2 and Cr doped TiO_2, PANI/ Cr-TiO_2 and pure polyaniline (PANI) at 1622cm^{-1}, 1515cm^{-1}, 1352cm^{-1}, and 1190cm^{-1} are respectively and it assigned to the stretching modes of C=C and C=N quinonoid units, benzenoid rings and in-plane bending vibration of C-H. In the spectrum of PANI/Cr-TiO_2 NTs, all these characteristics peaks of polyaniline are still existed except for a slight shift. The result suggest that the there might be a strong interaction between polyaniline and TiO_2 NTs [45]. Similarly, R. Dholam et al. (2009) studied about the FTIR spectra of Cr doped TiO_2 nanoparticles. The one distinct peak is at near about 430cm^{-1}, which is attributed to the vibration of TiO_2 units in anatase phase. The same

peak with more broadening also appears in low concentration (0.5-1at%) Cr doped TiO_2. It can be proved that the metal doping at low concentration, the TiO_2 anatase phase are still exist, but having a low crystalline degree. The vibration peak of anatase phase disappears in Cr doped TiO_2 films (2at%). By increasing the dopant concentration up to 5at% for the metal ion doping, the anatase phase related vibration peak disappears while a new peak at nearly about 490cm^{-1} emerges. This band has been assigned to the Ti-O-Ti stretching vibration in the rutile phase [46].

V. R. Akshay et al. (2019) showed the FTIR spectra of all the samples with increasing Cr content. The FTIR spectra have been taken for Cr doped TiO_2 nanocrystals because different types of functional group have been present in the sample. This functional group are associated with the organic solvent has been used in the synthetic process. A band at 847cm^{-1} is stretching vibration band associated with the Ti-O-Ti bonding. The shifting and broadening of the band position at 847cm^{-1} it confirms the presence of defects arising at a result of oxygen vacancies existing in the system due to Cr incorporation into the TiO_2 lattice. The symmetric and anti-symmetric stretching vibrations of the O-H functional groups were presented by the broad band at 4000-3200cm^{-1}. Bending vibration corresponding to the OH group appears between 1700 and 1300cm^{-1}, and this result showed adsorbed atmospheric water on the sample surface [47].

Surface Morphology

Cheng Chen et al. (2007) studied about the SEM images of 0.1% Zn doped TiO_2ste calcinated at 450°C and 0.1% Zn doped TiO_2sol calcinated at 450°C. Zn/TiO_2ste exhibited smaller crystallite agglomeration than Zn/TiO_2sol. The sample was prepared by steric acid gel method, $Ti(OC_4H_9)_4$ was dispersed in steric acid, preventing the particles from agglomerating; hence, smaller crystallite agglomerations were formed [25]. Thanh Binh Nguyen et al. (2011) studied the morphology of Zn doped TiO_2 sample was shown in figure. The particle size of the sample was about 15nm. The surfaces of the sample and particle size do not differ significantly so the SEM images of Zn/TiO_2 samples are shown. We have to increase the doping of Zn, the surface of the sample was the agglomeration. The entire sample used the same amount of ammonia at a controlled pH in the reaction. Therefore, the amount of Zn doping was increased, the pH decreased because the ammonia is diluted due to the additional water in zinc solution [26]. Similarly, Derya Kapusuz et al. (2013) and Chan-Soo Kim et al. (2012) also studied about the SEM images of Zr doped TiO_2 and Zr co-doped TiO_2 Nano-particles. The morphologies of the powder are quite similar. The powders are calcinated at 500°C exhibited spherical particles with quite rounded edges. A details look into the image can reveals the aggregation of crystallites. The aggregation is a considerable mode of anatase crystal growth in all the type of powders. The TiO_2 consisted of irregularly shaped particles with a wide size range (25-80nm) as shown in fig. The TiO_2 catalyst having no zirconium dopent featured non-uniform particles in large size (50-250nm), which was probably due to growth and densification of the dopant during calcination. The Zr doped TiO_2 formed relatively uniform particles (25-50nm) with some nano-agglomerates as shown in figure 3.

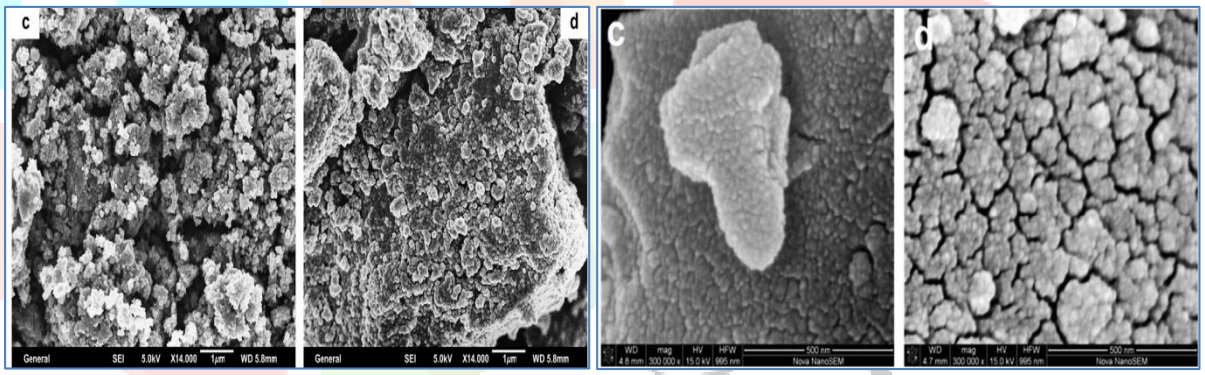

Figure.3 SEM image of (a) Zn doped TiO_2, (b) Zr doped TiO_2

The above figure 3 and figure 4 show the top view and cross-sectional SEM images of Zr doped TiO_2 and Polyaniline (PANI)/Cr-TiO_2 [30],[31]. The Nano-tubes are highly ordered and perpendicularly stand on the surface of titanium substrate, which is proved by Kun Yang et al. (2014). The length of the NPs are around 100nm-500nm and the outer diameter of the tube is about 30-35nm. The adsorption after polyaniline, many pieces of microcrystalline structured polyaniline is uniformly covered on the surface. The diameter of the particle does not show any changes, demonstrating that the morphology and structure of the Cr doped TiO_2 NPs are not influenced by the polyaniline [45]. R. Dholam et al. (2009) reported SEM cross-sectional micrograph of the metal doped TiO_2 thin film as shown in figure. A dense columnar structure is typically observed in Cr doped TiO_2 film deposited by sputtering. SEM images obtained in back sputtering mode, and it shows uniform distribution of metal ion in TiO_2 film [46].

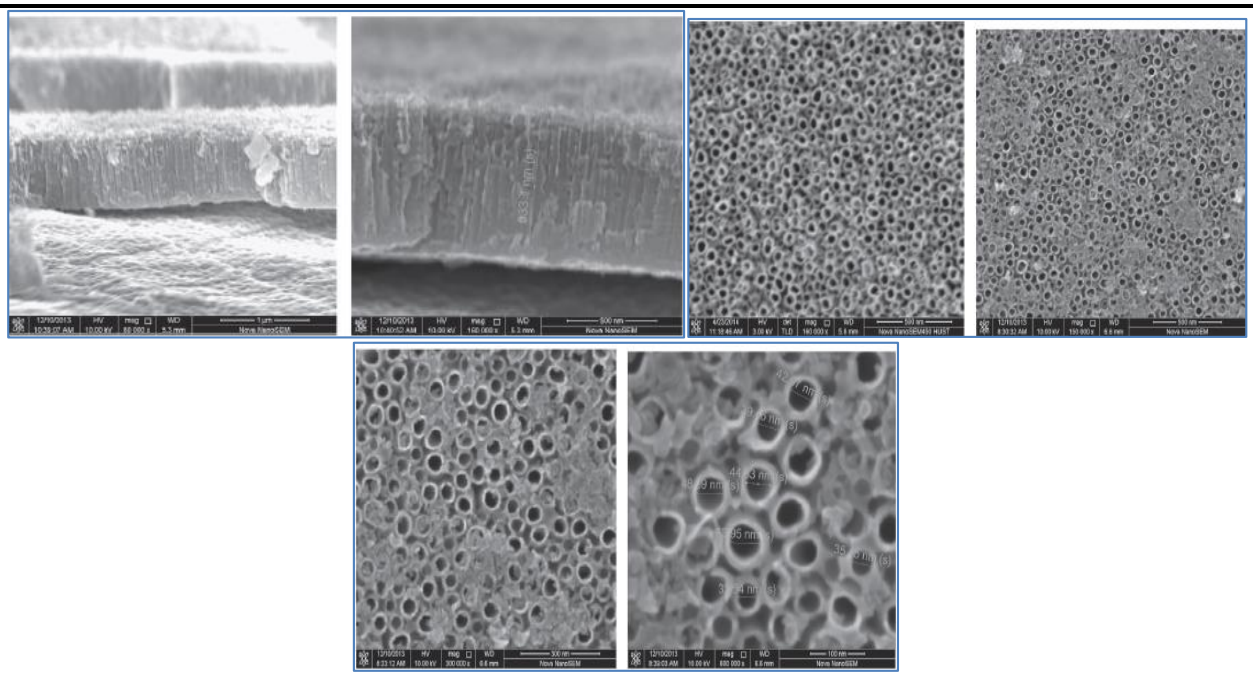

Figure.4 SEM image of Cr doped TiO_2

Ibrahim Elmehasseb et al. (2020) studied Transmission electron microscope (TEM) are essential tool for studying the surface morphology and shape of the prepared nanoparticles/nanocomposite. They also provide approximate measurement of the particle size, and it is a useful indication in the comparison between synthesized nanocatalysts. The prepared nanoparticles/nanocomposite has spherical shaped and aggregated with each other. Also, there is clearly defining particle size between them. TiO_2 nanoparticles are larger than that for Zn doped TiO_2 and N, S and Zn doped TiO_2 which becomes smaller and less agglomerated particles. For TiO_2, the obtained range was between (61-89nm), and the range was doped nanoparticles was between (42-70nm) and (26-45nm). The morphology proves the shape that detected from the TEM micrograph [27]. Same as Shuo Pang et al. (2016) showed TEM images of T-450, ZT-5-450 and HZT-1/9 it all shows the ordered porous structure of channel and it indicates they were consisted of highly crystalline and compact nanoparticles. The lattice spacing (0.35nm) matched the TiO_2 (101) crystallographic plane of the anatase TiO_2 in T-450. The lattice spacing was 0.32nm in ZT-5-450 it demonstrated Zn doping and the transformation from anatase phase to rutile phase. From the above result we can say that HZT-1/9 showed a better dispersion. A lattice spacing having 0.36nm which suggest H_2O_2 modification could inhibit the agglomeration of TiO_2 [14]. Sue-min Chang et al. (2009) HRTEM images of TOPO caped Zr doped TiO_2 nanocrystals calcinated at different temperature. The sample was calcinated at 450°C are still exhibited faceted roads, having length and width of ca 25.0 and 10.8nm. This type of faceted roads maintained shape and single-crystallinity up to 750°C, but few large particles were generated in irregular shapes in (fig c and e). The fused crystal boundaries were clearly shown in its high-magnification TEM images in (fig f). The surface of the sample was calcinated at 450 and 550°C were 112 and 114m^2/g. The surface area of TOPO capped Zr doped TiO_2 (0.5m^2/g) they were great increase in the specific surface area after calcination process were dur to removal of surface organic moieties and reduced the hydrophobic interaction between the nanocrystals. When the temperature was increased up to 750°C, heat-induced coalescence between particles reduced the specific surface are of sample to 57m^2/g. A smaller surface area of 2.4m^2/g was obtained after calcination at 950°C because of increased particle size [43].

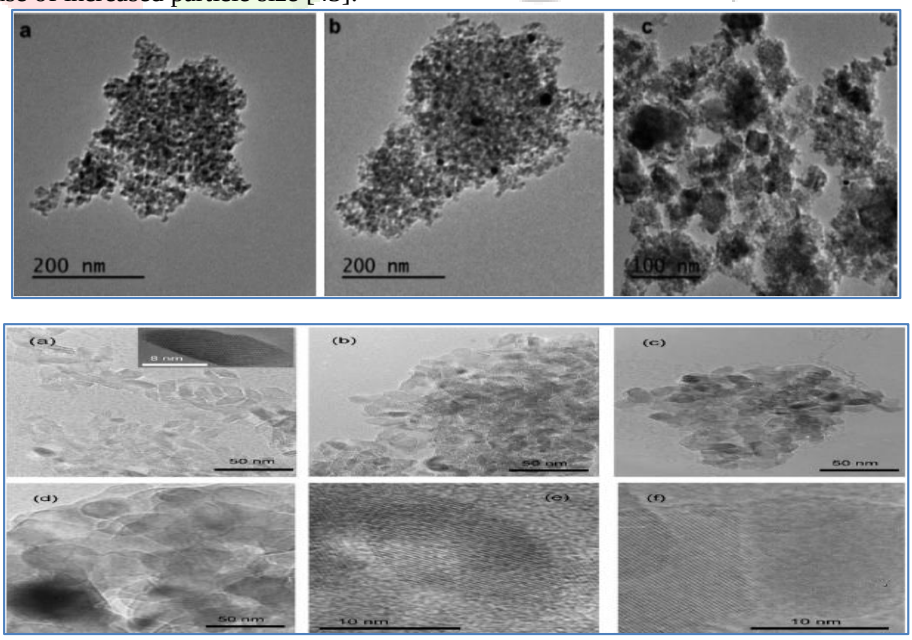

Figure.5 TEM images of (upper image) TiO_2, Zn doped TiO_2 and N, S and Zn doped TiO_2
TEM images of (lower image) TOPO caped Zr doped TiO_2 nanocrystals

Marc Estruga et al. (2010) showed several TEM micrograph of Zr doped TiO_2 powder. We have to analyse the selected area by electron diffraction pattern confirm that the TiO_2 phase present was anatase. Micrographs of Zr doped TiO_2 powder consists of roughly spherical nanocrystalline particles. The appearance and morphology of undoped titania were comparable with those of doped materials, indicating that low dopant content did not significantly affect titania morphology [44].

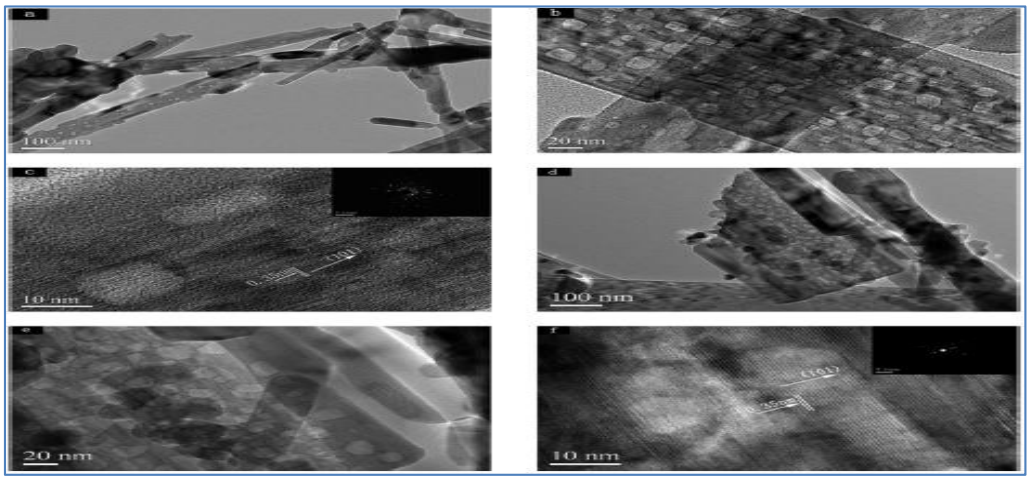

Figure.6 TEM images of undoped TiO_2 and 3mol% Cr doped TiO_2

The above figure represents the TEM images of TiO_2 and 3mol% Cr doped TiO_2 nanoroads after heating at 650°C, which is briefly studied by Hong Zhu et al. (2009). There are many types of nanocavities are present in the nanoroads shown in figure a and d. Figure b, e, the size of the nanocavities are 10-20nm in diameter and also these nanocavities have different shapes like circle, hexagon and rectangle. Figure c, f, represent the HR-TEM images of TiO_2 nanoroads with 0.35nm lattice spacing corresponding to the (101) crystal plane of anatase, and this was confirmed by the XRD result. The electron diffraction pattern are shown in the figure c, f indicates both undoped and doped anatase TiO_2 nanoroads posses the single crystalline structure. Some small aggregates are present on the surface of TiO_2 nanoroads in figure d and it can be shown that they were aggregates of small Cr_2O_3 particles. The size and quantity of the Cr_2O_3 particles are much smaller than those of TiO_2 nanoroads [33]. Similarly, E.D. Jeong et al. (2008) studied about the HRTEM images of Cr doped TiO_2 calcinated at 400°C. The average particle size of Cr doped TiO_2 nanoparticles is 21nm, in near agreement with the sizes estimated from XRD (ca. 18nm). The particle size of Cr doped TiO_2 nanoparticles were found to be similar as for the co-doped TiO_2 particles. The sample is consisted of fine particles yielding agglomerates of around 200nm. The particle size of metal doped TiO_2 prepared by hydrothermal treatment method was smaller than particles obtained by hydrolytic synthesis method [34].

Photo-catalytic Degradation Activity

Cheng Chen et al. (2007) studied about the photo-catalytic degradation activity. The absorption spectra of Zn doped TiO_2 calcinated at various temperatures as shown in fig 7. The amount of zinc dopant has not significant effect on the absorption band of Zn/TiO_2 prepared by stearic acid gel method. The band gap energy of the anatase and rutile phase of titania are 3.2eV and 3.0eV respectively. The absorption band of the rutile phase shifts to longer wavelength and observed absorption at higher wavelength may be ascribed to the increasing proportion of rutile phase. The 0.1% Zn doped TiO_2 Nano-crystals gives the best result of degradation of dye. The Zinc concentration below the optimal level, the improvement was observed in the photo-catalytic activity that accompanied by zinc doping can be explained by the zinc promotes the separation of electron hole pair in titania, since the doped ion can act as a separator of electron hole pairs. At Zinc concentration above the optimal level, the doped zinc ion can act as charge carrier recombination center; recombination of electron-hole pair increase with dopant concentration because of average distance between trap sites decreases with increases the number of dopant molecule confined within a particles [25].

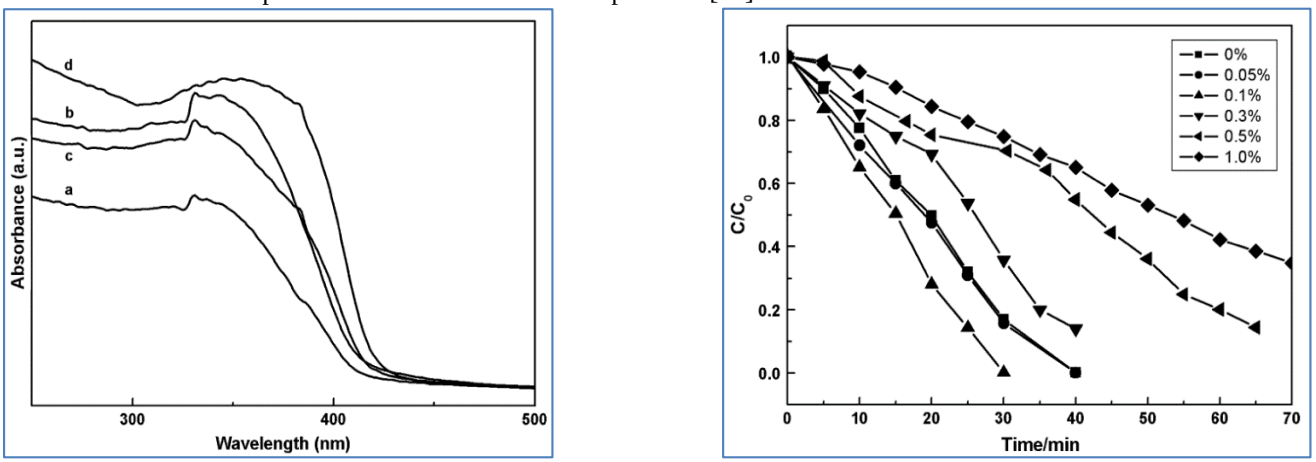

Figure.7: (a) UV absorption spectra of 0.1% Zn doped TiO_2 calcinated at various temperatures: 400°C, 450°C, 500°C, 600°C, (b)

Degradation profile for Zn doped TiO_2 nanocrystals calcinated at 450°C.

Thanh Binh Nguyen et al. (2011) premeditated about the photocatalytic degradation of Methylene Blue with the Zn doped TiO_2 nanocomposites. When the mol% of Zn ion doped in TiO_2 was increased, the photocatalytic activity was also increased. The photoreactivity of dopant metal ion of the TiO_2 is acting as electron or hole traps and by altering the e^-/h^+ pair recombination rate. The shifts of conduction band may accelerate the reduction while that of valance band may increase the oxidation reaction. Therefore, the

band gap energy of Zn doped TiO_2 is extremely small compared to pure TiO_2. The photocatalytic reaction may occur in the surface of semiconductor. An increase in the surface area and reduction in the particle size cause an increase in the photoactivity. If Zn doped TiO_2 sample has small particles size, reduced the recombination rates. The recombination was also affected by the defect factor, those of the Ti^{+3} and Zn ions [26]. Similarly, Ibrahim Elmehasseb et al. (2020) focused on the photodecomposition of methylene blue dye in waste water. Successfully removal of 5ppm dye in waste water, different amount of nanocrystals 3, 5, 7, 10, 15 and 20mg were used for degradation of organic dyes. The result of detoxification at 7mg dose is most suitable and active amount of nanocatalysts. Each catalyst of 7mg was used in a neutral medium under the illumination of visible light. By Zn doped TiO_2 the degradation process will completed in shorter time as degradation percent reached about 50% after 47minutes hence more activity. This process creates in the result of positive sites by holes and stream of aggressive electron, it cause the creation of hydroxyl radicals. The radicals attached to the organic pollutants and starts the oxidation mechanism which is characterized by high activity, complete degradation and safe products CO_2 and H_2O and some mineral acid depends on the chemical structure of the organic compounds [27].

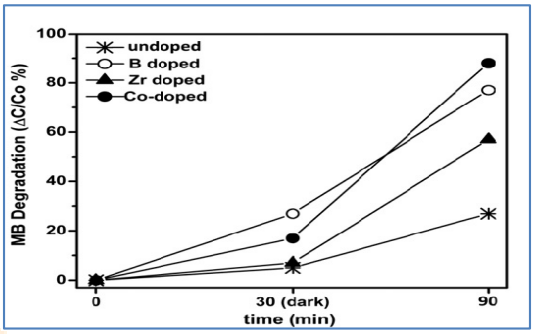

Figure.8 MB degradation of undoped, doped and B-Zr co-doped TiO_2 in 90minutes.

Derya Kapusuz et al. (2013) also studied the photocatalytic activity of MB of doped and co-doped TiO_2 nanocomposites in comparison to undoped TiO_2 after 30minutes of dark condition and 60minutes of UV radiation with a total testing time of 90minutes. The UV-vis absorption band of MB solution at 664nm decreased in intensity after doping/co-doping. Doping of TiO_2 was highly effective on degradation of MB dye in compare to the undoped TiO_2 has very low photocatalytical activity up to 27%. Zr co-doped powder represents the highest photocatalytic activity 88.5%. Zr ion with unoccupied 4d state above the lowest level of conduction band of TiO_2 improved photocatalytic activity. The smaller the crystallite size will get the higher the photo-catalytic activity owning to the decreased distance to the charge carrier to reach the surface without recombination. In case of co-doping, it can be suggested that higher photocatalytic activity was caused mainly by the synergetic effects of decreased crystallite size by doping and also increased lattice distortion. The result showed that synergetic effect of Zr ion on the electron hole makes the rate recombinant [30]. Same as, Chan-Soo Kim et al. (2012) compare the optical response of TiO_2, TiO_2/SiO_2 and $Zr/TiO_2/SiO_2$, UV-vis absorption spectra were taken. A shift of absorption spectrum to a lower energy region was observed for $Zr/TiO_2/SiO_2$. Absorption in the visible light range come from newly formed zirconium state that was incorporated into the lattice. The addition of zirconium have increased the surface acidity of TiO_2 catalyst through the formation of stronger surface OH group it act as a trap for holes and suppress the electron-hole recombination. To estimate the band gap energies, the absorption of sample were calculated by the equation:

$$Eg = 1240/\lambda g \qquad (3.2)$$

Where, λg is the overlap wavelength of the vertical and horizontal proportion of spectra. The absorption edge of TiO_2 was determined to be nearly 387.5nm with band gap of 3.2eV. Using four different plates gave total surface coating of catalyst of 37.5, 75, 112.5 and 150cm^2. The activity of $Zr/TiO_2/SiO_2$ catalyst was observed with the photo-oxidation medium of toluene and xylene under the UV and visible light. The maximum photodegradation efficiency at 150cm^2 towards toluene and xylene under UV light were 82% and 100%, while those under visible light irradiation were 30% and 68%. The efficiency of toluene and xylene photodegradation decreased with increasing initial toluene and xylene concentrations from 2.5 to 20ppm. Under the visible light the efficiency of toluene and xylene degradation increased remarkably (toluene from 10 to 27% and xylene from 8 to 50%) by adding additional lamps. Under UV light irradiation the amount of toluene and xylene can be absorbed on the active sites of the photocatalyst limited the performance; under visible light, there was not a limitation [31]. Baoqing Duan et al. (2018) observed the study of optical absorption behavior of Na-Zr/TiO_2 samples. The effects of adding Na on Zr/TiO_2 was characterized by a broad absorption at 2.87eV to 2.68eV. Because of Na^+ and Zr^{4+} were entered into TiO_2 lattice simultaneously, and an impurity level between conduction band and valance band is introduced. Therefore, it could be speculated that the position of conduction band decreased and unchanged in position of valance band. The sample reached its degradation limit after 24hours with lower catalytic degradation efficiency. Blue shifts of absorbance wavelength were observed and it indicates higher band gap energy. The Na-Zr/TiO_2 (0%) and Na-Zr/TiO_2 (2.5%) and commercial P25 catalyst were loaded in the box. After 60hours, the stable formaldehyde degradation rate of 83%, 95% and 78% were observed, and it shows the high capacity for formaldehyde degradation by Na doping [32].

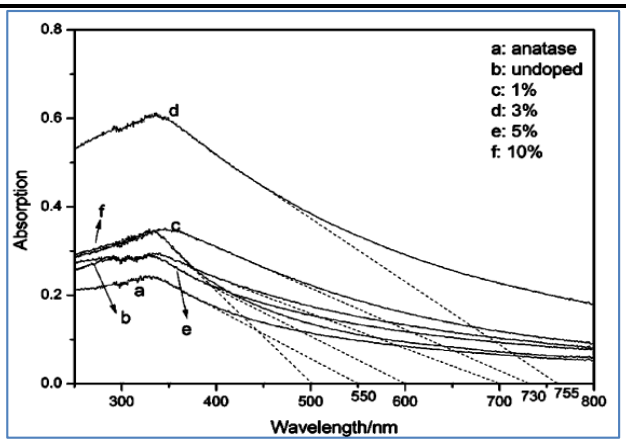

Figure.9 UV absorption spectra of doped TiO_2 NP (after heating at 650°C)

The above figure shows the UV-vis spectrum of different samples with the comparison of commercial anatase TiO_2 particles, the undoped and Cr-doped TiO_2 nanoroads exhibits a stronger absorption range of 250-400nm, which can be attributed to the backscattered light effects was observed by Nano-cavities. Hong Zhu et al. (2009) concluded from the absorption edges of anatase, undoped, 1% Cr-doped, 3% Cr-doped, 5% Cr-doped and 10% Cr-doped TiO_2 Nano-roads that the absorption edges of 1% and 3% Cr doped TiO_2 shifted to greater wavelength in the visible range, but 5% and 10% Cr doped TiO_2 nanoroads gives blue shifts compare to undoped TiO_2 nanoroads. Excessive amount of Cr is from deep dope levels, which are considered to be the recombination centers and they can accelerate recombination of electron-hole pairs. When the UV light is on, the photocurrent increases to steady state immediately. As the UV light is off, the change trends are different due to different bias potential. At the 0 V bias potential, the photocurrent of the sample decreases to a constant value in a few seconds. But at the 1.5 V bias potential, the photocurrent of 3mol% Cr doped TiO_2 Nano-roads decreases slowly. Cr doping can induce the separation of the electron and hole and prevents the electron-hole recombination, thus extending the life of the charge carrier [33]. The optical properties of pure and doped TiO_2 Nano-particles were examined by E.D. Jeong et al. (2008). The metal doped TiO_2, which exhibits larger absorption in the visible light region than other doped or pure TiO_2. The main absorption edge of TiO_2 was found out to be about 387nm (3.2eV). Cr and Fe doped TiO_2 show shoulders peak in the range of 450-700nm, which were absent in the spectrum of TiO_2. Cr^{3+} and Fe^{3+} ions shows strong absorption band in the UV region. The energy band gap of UV-vis spectra of doped TiO_2 and Cr and Fe co-doped TiO_2 are in the visible light region of 1.8-2.31eV. TiO_2 have no photocatalytic activity for IPA degradation to CO_2 under visible light. But, doped and pure TiO_2 show the activity for IPA degradation to CO_2. The Cr and Fe co-doped TiO_2 showed much higher decomposition rates and activities than those of Cr/Fe doped TiO_2 for IPA degradation. Thus, the materials have co-doped with Cr and Fe exhibit two more times higher photocatalytic activity for photodecomposition of IPA gases than Cr/Fe doped particles under visible light [34].

Yan-Hua Peng et al. (2010) were also pragmatic the increasing concentration of Cr, which shows a shift in the absorption bandedge towards longer wavelength. At 0.2M Cr concentration, the red shifts of absorption bandedge reach its maximum of about 800nm. Absorption at wavelength of less than 387nm is caused by the intrinsic band gap absorption of TiO_2. The origin of visible light sensitivity in Cr doped TiO_2 can be ascribed to the appearance of additional energy level such as Cr 2p level and oxygen vacancies within the band gap of TiO_2 due to the Cr doping. In the level of Cr 2p, oxygen vacancies also played an important role in enhancement of visible-light absorption. Moreover, oxygen vacancies are introduced into the lattice of TiO_2 with Cr doping. It can be reported that the oxygen vacancy states is located between 0.75eV-1.2eV. Below the conduction band of TiO_2, the band due to the formation of oxygen vacancies induce the visible light absorption ranging from 500-600nm of TiO_2. When the concentration of Cr is higher or about 0.3M, the solution is not stable, leading to the low efficiency on doping Cr into TiO_2 lattice. Cr doped TiO_2 provides much higher efficiency for methyl orange photo-degradation; it indicates that appropriate Cr doping could greatly improve the photocatalytic activity of TiO_2. Oxygen vacancy in TiO_2 can act as electron trap and which can bind the photoinduced electron and plays a major role in inhibiting the recombination rate of photoinduced electron-hole pairs, thus enhancing the photocatalytic activity of TiO_2. Cr doped TiO_2 nanocrystal films used widely in practical applications as photocatalytic materials to decompose hazardous organic pollutants in contaminated water [22].

IV. CONCLUSION

Metal doped metal oxides Nano-composites have various applications in different fields. It has been proved with this literature survey that to synthesis these types of Nano-composites, sol-gel method is an accurate and precise technique to be applied. Here, the literature survey shows various applications of three different Nano-composites (Zr doped TiO_2, Cr doped TiO_2 and Zn doped TiO_2 Nano-composites). With the help of literature survey, it has been approved that metal doped metal oxides Nano-composites can be perfectly synthesised by sol-gel method. Metal doped metal oxides have many diverse properties, which can be used in so many ways. With the help of these Nano-composites, dye degradation process has been done with photo-catalytic process. By comparing these three Nano-composites, it is clearly shown that Zn doped TiO_2 and Cr doped TiO_2 are being widely useful to detect various organic and inorganic contaminations in water and other liquid compounds. By the literature survey, it has been proved that Zn doped TiO_2 and Cr doped TiO_2 have good properties to detect contamination in less time by photo-catalytic process, which shows the quenching study of the main solutions. Zn doped TiO_2 and Cr doped TiO_2 have their band gaps between 1.5eV to 2.35eV, which helps to attract the other materials to share their atoms. With the help of UV-Vis-Spectrometer, the quenching study of dye degradation with metal doped metal oxides Nano-composites has been studied to detect the hazardous materials in liquid solution. This literature survey also concluded that there are numbers of parameters like NP calcinations temperature, weight by volume ratio of Nano-particle in Nano-composites, different solvent, etc., which can be measured or matter during the experiments and it shows different results with different parameters and applications.

V. REFERENCES

[1] C. C. Okpala, "Nanocomposites – An Overview," *Int. J. Eng. Res. Dev.*, vol. 8, no. 11, pp. 17–23, 2013.

[2] M. F.-G. and J. A. Rodriguez, "Metal Oxide Nanoparticles," *Encycl. Inorg. Chem.*, no. October, 2009, doi: 10.1002/0470862106.ia377.

[3] V. T. Rathod, J. S. Kumar, and A. Jain, "Polymer and ceramic nanocomposites for aerospace applications," *Appl. Nanosci.*, vol. 7, no. 8, pp. 519–548, 2017, doi: 10.1007/s13204-017-0592-9.

[4] C. Chikwendu Okpala, "the Benefits and Applications of Nanocomposites," *Int. J. Adv. Eng. Technol. E- Int J Adv Engg Tech*, pp. 12–18, 2006.

[5] H. Gu *et al.*, "An overview of multifunctional epoxy nanocomposites," *J. Mater. Chem. C*, vol. 4, no. 25, pp. 5890–5906, 2016, doi: 10.1039/c6tc01210h.

[6] J. Njuguna, K. Pielichowski, and J. Fan, *Polymer nanocomposites for aerospace applications*. Woodhead Publishing Limited, 2012.

[7] P. Xu, X. Han, B. Zhang, Y. Du, and H. L. Wang, "Multifunctional polymer-metal nanocomposites via direct chemical reduction by conjugated polymers," *Chem. Soc. Rev.*, vol. 43, no. 5, pp. 1349–1360, 2014, doi: 10.1039/c3cs60380f.

[8] A. Lateef and R. Nazir, "Metal Nanocomposites : Synthesis , Characterization and their Applications," *Sci. Appl. Tailored Nanostructures*, pp. 239–256, 2017.

[9] N. Patelli, A. Migliori, V. Morandi, and L. Pasquini, "One-step synthesis of metal/oxide nanocomposites by gas phase condensation," *Nanomaterials*, vol. 9, no. 2, pp. 1–15, 2019, doi: 10.3390/nano9020219.

[10] P. H. C. Camargo, K. G. Satyanarayana, and F. Wypych, "Nanocomposites: Synthesis, structure, properties and new application opportunities," *Mater. Res.*, vol. 12, no. 1, pp. 1–39, 2009, doi: 10.1590/S1516-14392009000100002.

[11] J. Li, S. Tang, L. Lu, and H. C. Zeng, "Preparation of nanocomposites of metals, metal oxides, and carbon nanotubes via self-assembly," *J. Am. Chem. Soc.*, vol. 129, no. 30, pp. 9401–9409, 2007, doi: 10.1021/ja071122v.

[12] C. Douce, P. Sol, and G. Product, "SOL-GEL PROCESS," pp. 40–77.

[13] M. J. Pawar and V. B. Nimbalkar, "Synthesis and phenol degradation activity of Zn and Cr doped TiO 2 Nanoparticles," *Res. J. Chem. Sci.*, vol. 2, no. 1, pp. 3–8, 2012.

[14] S. Pang *et al.*, "Synthesis and Modification of Zn-doped TiO2 Nanoparticles for the Photocatalytic Degradation of Tetracycline," *Photochem. Photobiol.*, vol. 92, no. 5, pp. 651–657, 2016, doi: 10.1111/php.12626.

[15] G. Liu, X. Zhang, Y. Xu, X. Niu, L. Zheng, and X. Ding, "The preparation of Zn2+-doped TiO2 nanoparticles by sol-gel and solid phase reaction methods respectively and their photocatalytic activities," *Chemosphere*, vol. 59, no. 9, pp. 1367–1371, 2005, doi: 10.1016/j.chemosphere.2004.11.072.

[16] Y. S. Tamgadge, G. G. Muley, K. U. Deshmukh, and V. G. Pahurkar, "Synthesis and nonlinear optical properties of Zn doped TiO2 nano-colloids," *Opt. Mater. (Amst).*, vol. 86, no. July, pp. 185–190, 2018, doi: 10.1016/j.optmat.2018.09.030.

[17] S. Naraginti, F. B. Stephen, A. Radhakrishnan, and A. Sivakumar, "Zirconium and silver co-doped TiO2 nanoparticles as visible light catalyst for reduction of 4-nitrophenol, degradation of methyl orange and methylene blue," *Spectrochim. Acta - Part A Mol. Biomol. Spectrosc.*, vol. 135, pp. 814–819, 2015, doi: 10.1016/j.saa.2014.07.070.

[18] J. Wang, Y. Yu, S. Li, L. Guo, E. Wang, and Y. Cao, "Doping behavior of Zr4+ ions in Zr4+-doped TiO 2 nanoparticles," *J. Phys. Chem. C*, vol. 117, no. 51, pp. 27120–27126, 2013, doi: 10.1021/jp407662d.

[19] B. Gao, T. M. Lim, D. P. Subagio, and T. T. Lim, "Zr-doped TiO2 for enhanced photocatalytic degradation of bisphenol A," *Appl. Catal. A Gen.*, vol. 375, no. 1, pp. 107–115, 2010, doi: 10.1016/j.apcata.2009.12.025.

[20] T. Bigdeli and S. Moradi Dehaghi, "The effect of trace amount of Zr-doped TiO2 on photocatalytic activity in degradation of organic waste," *Energy Sources, Part A Recover. Util. Environ. Eff.*, vol. 40, no. 3, pp. 274–281, 2018, doi: 10.1080/15567036.2017.1300960.

[21] B. Choudhury and A. Choudhury, "Structural, optical and ferromagnetic properties of Cr doped TiO 2 nanoparticles," *Mater. Sci. Eng. B Solid-State Mater. Adv. Technol.*, vol. 178, no. 11, pp. 794–800, 2013, doi: 10.1016/j.mseb.2013.03.016.

[22] Y. H. Peng, G. F. Huang, and W. Q. Huang, "Visible-light absorption and photocatalytic activity of Cr-doped TiO 2 nanocrystal films," *Adv. Powder Technol.*, vol. 23, no. 1, pp. 8–12, 2012, doi: 10.1016/j.apt.2010.11.006.

[23] C. C. Pan and J. C. S. Wu, "Visible-light response Cr-doped TiO2-XNX photocatalysts," *Mater. Chem. Phys.*, vol. 100, no. 1, pp. 102–107, 2006, doi: 10.1016/j.matchemphys.2005.12.013.

[24] C. Wang, H. Shi, and Y. Li, "Synthesis and characterization of natural zeolite supported Cr-doped TiO 2 photocatalysts," *Appl. Surf. Sci.*, vol. 258, no. 10, pp. 4328–4333, 2012, doi: 10.1016/j.apsusc.2011.12.108.

[25] C. Chen, Z. Wang, S. Ruan, B. Zou, M. Zhao, and F. Wu, "Photocatalytic degradation of C . I . Acid Orange 52 in the presence of Zn-doped TiO 2 prepared by a stearic acid gel method," *ScienceDirect*, vol. 77, pp. 204–209, 2008, doi: 10.1016/j.dyepig.2007.05.003.

[26] T. B. Nguyen, M.-J. Hwang, and K.-S. Ryu, "Synthesis and High Photocatalytic Activity of Zn-doped TiO 2 Synthesis and High Photocatalytic Activity of Zn-doped TiO ...," *Bull. Korean Chem. Soc.*, vol. 33, no. January, pp. 1–5, 2012, doi: 10.5012/bkcs.2012.33.1.243.

[27] I. Elmehasseb, S. Kandil, and K. Elgendy, "Optik Advanced visible-light applications utilizing modified Zn-doped TiO 2 nanoparticles via non-metal in situ dual doping for wastewater detoxification," *Opt. - Int. J. Light Electron Opt.*, vol. 213, no. November 2019, p. 164654, 2020, doi: 10.1016/j.ijleo.2020.164654.

[28] C. M. Malengreaux, S. L. Pirard, J. R. Bartlett, and B. Heinrichs, "Kinetic study of 4-nitrophenol photocatalytic degradation over a Zn 2 + doped TiO 2 catalyst prepared through an environmentally friendly aqueous sol – gel process," *Chem. Eng. J.*, vol. 245, pp. 180–190, 2014, doi: 10.1016/j.cej.2014.01.068.

[29] N. Prabhakarrao, M. R. Chandra, and T. S. Rao, "SC," *J. Alloys Compd.*, 2016, doi: 10.1016/j.jallcom.2016.09.329.

[30] D. Kapusuz, J. Park, and A. Ozturk, "Journal of Physics and Chemistry of Solids Sol – gel synthesis and photocatalytic activity of B and Zr co-doped TiO 2," *J. Phys. Chem. Solids*, vol. 74, pp. 1026–1031, 2013, doi: 10.1016/j.jpcs.2013.02.022.

[31] C. Kim, J. Shin, S. An, H. Jang, and T. Kim, "Photodegradation of volatile organic compounds using zirconium-doped TiO 2 / SiO 2 visible light photocatalysts," *Chem. Eng. J.*, vol. 204–206, pp. 40–47, 2012, doi: 10.1016/j.cej.2012.07.093.

[32] B. Duan, Y. Zhou, C. Huang, Q. Huang, H. Xu, and S. Shen, "Kinetics , Catalysis , and Reaction Engineering Impact of Zr-doped-TiO2 photocatalyst on formaldehyde degradation by Na addition," *Am. Chem. Soc. 1155 Sixt. Str. N.W., Washington, DC 20036*, 2018, doi: 10.1021/acs.iecr.8b03016.

[33] and X. D. Hong Zhu, Jie Tao, "Preparation and Photoelectrochemical Activity of Cr-Doped TiO 2 Nanorods with Nanocavities," *J. Phys. Chem.*, pp. 2873–2879, 2010.
[34] E. D. Jeong *et al.*, "Hydrothermal synthesis of Cr and Fe co-doped TiO 2 nanoparticle photocatalyst," *J. Ceram. Process. Res.*, no. October, 2013.
[35] S. Chen, W. Zhao, W. Liu, and S. Zhang, "Preparation, characterization and activity evaluation of p-n junction photocatalyst p-ZnO/n-TiO 2," *Appl. Surf. Sci.*, vol. 255, no. 5 PART 1, pp. 2478–2484, 2008, doi: 10.1016/j.apsusc.2008.07.115.
[36] Y. Zhao, C. Li, X. Liu, F. Gu, H. L. Du, and L. Shi, "Zn-doped TiO2 nanoparticles with high photocatalytic activity synthesized by hydrogen-oxygen diffusion flame," *Appl. Catal. B Environ.*, vol. 79, no. 3, pp. 208–215, 2008, doi: 10.1016/j.apcatb.2007.09.044.
[37] D. A. T. Akira Fujishima, Tata N. Rao, "Titanium dioxide photocatalysis," *J. Photochem. Photobiol.*, vol. 1, no. 2000, pp. 1–21, 2000.
[38] J. Lukáč *et al.*, "Influence of Zr as TiO2 doping ion on photocatalytic degradation of 4-chlorophenol," *Appl. Catal. B Environ.*, vol. 74, no. 1–2, pp. 83–91, 2007, doi: 10.1016/j.apcatb.2007.01.014.
[39] R. Saravanan, S. Karthikeyan, V. K. Gupta, G. Sekaran, V. Narayanan, and A. Stephen, "Enhanced photocatalytic activity of ZnO/CuO nanocomposite for the degradation of textile dye on visible light illumination," *Mater. Sci. Eng. C*, vol. 33, no. 1, pp. 91–98, 2013, doi: 10.1016/j.msec.2012.08.011.
[40] K. Kaviyarasu *et al.*, "In vitro cytotoxicity effect and antibacterial performance of human lung epithelial cells A549 activity of Zinc oxide doped TiO2 nanocrystals: Investigation of bio-medical application by chemical method," *Mater. Sci. Eng. C*, vol. 74, pp. 325–333, 2017, doi: 10.1016/j.msec.2016.12.024.
[41] A. Stoyanova, H. Hitkova, A. Bachvarova-Nedelcheva, R. Iordanova, N. Ivanova, and M. Sredkova, "Synthesis and antibacterial activity of TiO2/ZnO nanocomposites prepared via nonhydrolytic route," *J. Chem. Technol. Metall.*, vol. 48, no. 2, pp. 154–161, 2013.
[42] L. ying QIAO, F. yu XIE, M. hui XIE, C. hua GONG, W. lang WANG, and J. cheng GAO, "Characterization and photoelectrochemical performance of Zn-doped TiO2 films by sol–gel method," *Trans. Nonferrous Met. Soc. China (English Ed.*, vol. 26, no. 8, pp. 2109–2116, 2016, doi: 10.1016/S1003-6326(16)64325-X.
[43] S. min Chang, C. yao Hou, P. han Lo, and C. tuan Chang, "Preparation of phosphated Zr-doped TiO2 exhibiting high photocatalytic activity through calcination of ligand-capped nanocrystals," *Appl. Catal. B Environ.*, vol. 90, no. 1–2, pp. 233–241, 2009, doi: 10.1016/j.apcatb.2009.03.009.
[44] M. Estruga, C. Domingo, X. Domènech, and J. A. Ayllón, "Zirconium-doped and silicon-doped TiO2 photocatalysts synthesis from ionic-liquid-like precursors," *J. Colloid Interface Sci.*, vol. 344, no. 2, pp. 327–333, 2010, doi: 10.1016/j.jcis.2009.12.063.
[45] K. Yang, W. Pu, Y. Tan, M. Zhang, C. Yang, and J. Zhang, "Enhanced photoelectrocatalytic activity of Cr-doped TiO2 nanotubes modified with polyaniline," *Mater. Sci. Semicond. Process.*, vol. 27, pp. 777–784, 2014, doi: 10.1016/j.mssp.2014.08.007.
[46] R. Dholam, N. Patel, M. Adami, and A. Miotello, "Hydrogen production by photocatalytic water-splitting using Cr- or Fe-doped TiO2 composite thin films photocatalyst," *Int. J. Hydrogen Energy*, vol. 34, no. 13, pp. 5337–5346, 2009, doi: 10.1016/j.ijhydene.2009.05.011.
[47] V. R. Akshay, B. Arun, G. Mandal, and M. Vasundhara, "Visible range optical absorption, Urbach energy estimation and paramagnetic response in Cr-doped TiO2 nanocrystals derived by a sol-gel method," *Phys. Chem. Chem. Phys.*, vol. 21, no. 24, pp. 12991–13004, 2019, doi: 10.1039/c9cp01351b.